Rapid Detection of Melamine in Tap Water and Milk Using Conjugated "One-Step" Molecularly Imprinted Polymers-Surface Enhanced Raman Spectroscopic Sensor

Yaxi Hu and Xiaonan Lu

Abstract: An innovative "one-step" sensor conjugating molecularly imprinted polymers and surface enhanced Raman spectroscopic-active substrate (MIPs-SERS) was investigated for simultaneous extraction and determination of melamine in tap water and milk. This sensor was fabricated by integrating silver nanoparticles (AgNPs) with MIPs synthesized by bulk polymerization of melamine (template), methacrylic acid (functional monomer), ethylene glycol dimethacrylate (cross-linking agent), and 2,2'-azobisisobutyronitrile (initiator). Static and kinetic adsorption tests validated the specific affinity of MIPs-AgNPs to melamine and the rapid adsorption equilibration rate. Principal component analysis segregated SERS spectral features of tap water and milk samples with different melamine concentrations. Partial least squares regression models correlated melamine concentrations in tap water and skim milk with SERS spectral features. The limit of detection (LOD) and limit of quantification (LOQ) of melamine in tap water were determined as 0.0019 and 0.0064 mmol/L, while the LOD and LOQ were 0.0165 and 0.055 mmol/L for the determination of melamine in skim milk. However, this sensor is not ideal to quantify melamine in tap water and skim milk. By conjugating MIPs with SERS-active substrate (that is, AgNPs), reproducibility of SERS spectral features was increased, resulting in more accurate detection. The time required to determine melamine in tap water and milk were 6 and 25 min, respectively. The low LOD, LOQ, and rapid detection confirm the potential of applying this sensor for accurate and high-throughput detection of melamine in tap water and milk.

Keywords: chemometrics, food adulteration, melamine, molecular imprinting, Raman spectroscopy

Practical Application: A new method for rapid detection of melamine in tapping water and milk.

Introduction

Melamine, an industrial material used for the production of melamine resins, was added deliberately to protein-rich foods for economically motivated adulteration. Containing 66.7% nitrogen by weight, melamine increases the amount of apparent protein content determined by nonspecific Kjeldahl method, which assumes that all nitrogen content comes from protein. Although melamine itself has low toxicity, it could be hydrolyzed to cyanuric acid in body and form low soluble crystals with cyanuric acid, resulting in renal failure (Li and others 2015), which caused thousands of injuries and deaths of babies and pets after consuming melamine adulterated infant formula and pet foods, respectively (Brown and others 2007; Wu and others 2009). Proposed by World Health Organization, the maximum tolerance of melamine concentration allowed in dried infant formula and other products containing milk are 1 parts per million (ppm) and 2.5 ppm (Ingelfinger 2008), respectively. The "baseline" level of melamine in processed foods can be attributed to the widespread uses of melamine in resin production and fertilizer, leading to the contamination of soil and water. To assure the conformance with these regulations and monitor melamine level in the environmental sources, rapid and accurate determination techniques with specificity to melamine are highly demanded.

Commonly employed approaches for the determination of melamine involve solid phase extraction (SPE) or liquid–liquid extraction to remove sample matrices, and liquid chromatography or gas chromatography for further separation of melamine from impurities, followed by a detection technique such as mass spectrometer or photo-diode array detector (DAD) (Xu and others 2009; Filazi and others 2012; Zheng and others 2012). Although low limit of detection (LOD) and limit of quantification (LOQ) can be achieved with these aforementioned techniques, the overall analyses are time consuming, expensive, labor intensive, and need highly trained personnel to perform complicated instruments. These attributes interfere with the high-throughput screening required by food industry and government laboratory.

As a non- or less-destructive detection method (Li-Chan 1996; Choo-Smith and others 2002; Gao and others 2014), Raman spectroscopy can be applied without any sample pretreatment or analyte extraction procedures and the instrumentation operation is simple and rapid. Raman spectroscopy reflects vibrational modes associated with functional groups in chemicals, providing unique inelastic Raman scattering pattern for each chemical (Colthup 2012). In addition, melamine is a Raman-active molecule with a unique Raman band at the wavenumber of 674 cm^{-1}, making it applicable to be sensed by Raman spectrometer. However,

MS 20151994 Submitted 12/1/2015, Accepted 2/25/2016. *Authors are with Food, Nutrition and Health Program, Faculty of Land and Food Systems, The Univ. of British Columbia, Vancouver, BC, V6T 1Z4, Canada. Direct inquiries to author Lu (E-mail: xiaonan.lu@ubc.ca).*

Journal of Food Science A Publication of the Institute of Food Technologists

doi: 10.1111/1750-3841.13283

because of the weak inelastic Raman scattering (Lu and others 2012), traditional Raman spectroscopy is not applicable for trace-level detection of food chemical hazards. With the assistance of noble metallic (for example, silver or gold) nanostructure (that is, SERS-active substrate), surface enhanced Raman spectroscopy (SERS) is a technique that can enhance faint Raman cross section significantly when the chemical approaches to the electromagnetic field on the surface of SERS-active substrate, resulting in the detection of single molecules (Lu and others 2013). Based on the advantages of SERS, it is an emerging technique to be applied in the detection of food chemical hazards (Cheung and others 2010; Xie and others 2012; Liu and others 2013).

However, effective and efficient sample pretreatment or analyte extraction is still required because SERS collects scattering signals from every chemical appeared in the sample, which hinders the accuracy of detection. By applying extraction techniques with specificity to target analyte, removal of the food matrices can be achieved more efficiently. Techniques involving antibody and "artificial antibody" [that is, aptamer and molecularly imprinted polymers (MIPs)] are candidates (He and others 2007, 2011a, b; Yakala and others 2013; Pang and others 2014). Although protein-based antibody and DNA-based aptamer have higher specificity and sensitivity to target analyte than polymer-based MIPs, the production procedures for those 2 are more complicated than that of MIPs. In addition, the type of the target analyte that can be recognized by antibody and aptamer is very limited, constraining their wide usage. Moreover, antibody is very sensitive and degraded easily in the harsh conditions (for example, extreme temperature or extreme *p*H), which is not desirable for in-field application. Therefore, MIPs, which is simple to be synthesized, stable in the extreme conditions and has specificity toward a wide range of chemicals (Wang and others 2007; He and others 2008; Yang and others 2009; Lombardo-Agüí and others 2010), is more suitable to be used in the determination of food chemical hazards. The synthesis of MIPs involves the copolymerization of functional monomer and cross-linking agents, forming rigid shell around target analyte which is used as the template (Haupt 2003). After removal of the template, cavities imprinted with the chemical and physical properties of template are exposed. Thus, MIPs can be used to exclusively recognize and bind to target analyte, achieving a high efficiency to simultaneously extract analyte and remove impurities.

Recent studies have demonstrated the feasibility of combining MIPs with SERS for extraction and detection of target analyte in food systems. Strategies to integrate these 2 techniques can be divided into 2 categories: "two-step" and "one-step" MIPs-SERS sensor. Recent publications validated the potential of using MIPs as specific sorbent in SPE to extract target analyte, and silver dendrite as SERS-active substrate to enhance Raman scattering of the eluent from SPE (Feng and others 2013; Gao and others 2014; Hu and others 2015). These sensors contain 2 sensing elements (that is MIPs and SERS-active substrate) are regarded as "two-step" MIPs-SERS sensor. However, the SERS spectral reproducibility of the "two-step" sensor is not ideal because variations exist in the synthesis of SERS-active substrates, leading to variances in the shape and intensity of the electromagnetic field. By depositing the liquid samples onto the substrates, the final location of molecules on the substrate is random as well, due to the Brownian movement.

"One-step" MIPs-SERS sensors for theophylline (Liu and others 2011), TNT (Holthoff and others 2011), and S-propranolol (Kantarovich and others 2010) have been successfully fabricated by conjugating MIPs with different SERS-active substrates. Through developing MIPs on the surface of SERS-active substrates or with the substrates incorporated in during polymerization, locations of the substrates on MIPs are fixed. Thus, distances between the cavities for analyte in MIPs and the substrates can be precisely controlled. Consequently, analyte adsorbed onto MIPs also located closely to SERS-active substrates (<10 nm), resulting in improved reproducibility of SERS spectra. The methodology proposed by Liu and others (2011) integrated AgNPs with MIPs by adding silver nitrate as AgNPs precursor that bind to theophylline during bulk polymerization. Melamine contains a triazine ring, which is similar to the imidazole structure in theophylline that interacted with AgNPs precursor during polymerization. Therefore, this methodology was adopted in this study.

The objective of the current study was to develop a "one-step" MIPs-SERS sensor for rapid detection of melamine in tap water and milk by using AgNPs incorporated MIPs synthesized by bulk polymerization for simultaneous extraction and detection. To the best of our knowledge, this was the first study investigating "one-step" MIPs-SERS sensor for high-throughput screening of melamine in water and foods.

Materials and Methods

Chemicals and reagents

Methacrylic acid (MAA), ethylene glycol dimethacrylate (EGDMA), 2,2'-azobis(isobutyronitrile) (AIBN), melamine, silver nitrite ($AgNO_3$), sodium borohydride ($NaBH_4$), and zinc plate were purchased from Sigma-Aldrich (St. Louis, Mo., U.S.A.). Methanol (HPLC grade), acetonitrile (HPLC grade), ethanol (HPLC grade), ammonium hydroxide, and acetic acid were purchased from Thermo Fisher Scientific (Toronto, ON, Canada). Tap water was collected from local home and skim milk samples were obtained from local grocery stores. Melamine stock solution (1 mmol/L) was prepared in methanol, stored at 20 °C, and diluted by methanol for further use as working solution.

Synthesis of MIPs-AgNPs

The synthesis of MIPs-AgNPs for melamine followed the procedures by Hu and others (2015) with modifications. Briefly, 0.5 mmol of melamine (template) was dissolved in 5 mL of ethanol and 1.5 mL of water (porogen). After adding 6 mmol of MAA (functional monomer), the mixture was magnetically stirred for 10 min. Then 30 mmol of EGDMA (cross-linker) was added, followed by incubation at 50 °C in oil bath overnight. Subsequently, 500 mg $AgNO_3$ (AgNPs precursor) and 0.25 mmol of AIBN were added, and the mixture was purged with nitrogen for 10 min. The solution was sealed and incubated for 24 h at 60 °C in oil bath. The monolithic product was ground and sieved through a 200 mesh steel sieve to obtain homogeneous fine particles. Before applying Soxhlet extraction to remove template, excessive $NaBH_4$ was added to reduce MIPs-$AgNO_3$ into MIPs-AgNPs. Soxhlet extraction was conducted using 250 mL of methanol/acetic acid (8:2, v/v) for 24 h, and another 250 mL of methanol was used for further extraction. Finally, the MIPs were dried for 12 h in a vacuum drying oven at 50 °C. The nonimprinted polymers (NIPs-AgNPs) was synthesized following the same procedure without addition of template (that is, melamine).

Raman spectra of MIPs-AgNPs and NIPs-AgNPs were collected to confirm the success of AgNPs formation and the complete removal of template molecule (melamine). MIPs-AgNPs before and after the reduction were also scanned by UV-Vis spectrometer to confirm the formation of AgNPs. MIPs synthesized

recently in our laboratory for melamine "two-step" MIPs-SERS sensor (Hu and others 2015) was used as no-AgNPs control.

Adsorption capacity tests

Static and kinetic adsorption tests were conducted to confirm the specific affinity of MIPs-AgNPs toward melamine and the equilibration rates. For static adsorption test, 10 mg of MIPs-AgNPs or NIPs-AgNPs was mixed with 2 mL melamine standard solutions at selective concentrations ranging from 0.01 to 0.2 mmol/L. The mixtures were horizontally shaken for 2 h at 20 °C. After centrifugation at 12000 × *g* for 3 min, the supernatant was filtered through a 0.22-μm nylon syringe filter (Thermo Scientific, Rockwood, Tenn., U.S.A.), and the final concentration of melamine was determined by high-performance liquid chromatography (HPLC) with DAD set at a wavelength of 240 nm. The pellet (that is, MIPs-AgNPs and NIPs-AgNPs) was deposited onto gold-coated microarray for Raman spectral collection.

Kinetic adsorption test was conducted by mixing 10 mg MIPs or NIPs with 2 mL melamine solution (0.1 mmol/L). The mixtures were horizontally shaken for different time intervals ranging from 5 to 90 min. After the centrifugation at 12000 × *g* for 3 min, the supernatant and pellet were treated and determined following the same procedures as static adsorption aforementioned.

Skim milk sample pretreatment

Skim milk was spiked with different concentrations of melamine ranging from 0.01 to 1 mmol/L. Nonspecific sample pretreatment was conducted by using Phenomenex Strate Melamine SPE cartridge (silica-based sorbent) to partially remove milk matrices. Briefly, 1 mL of milk was mixed with 3 mL of acetonitrile. After shaking for 10 s, the mixture was centrifuged at 8000 × *g* for 5 min. An aliquot of 2 mL of the supernatant were loaded onto SPE cartridge. After washing with 1 mL 50% acetonitrile and

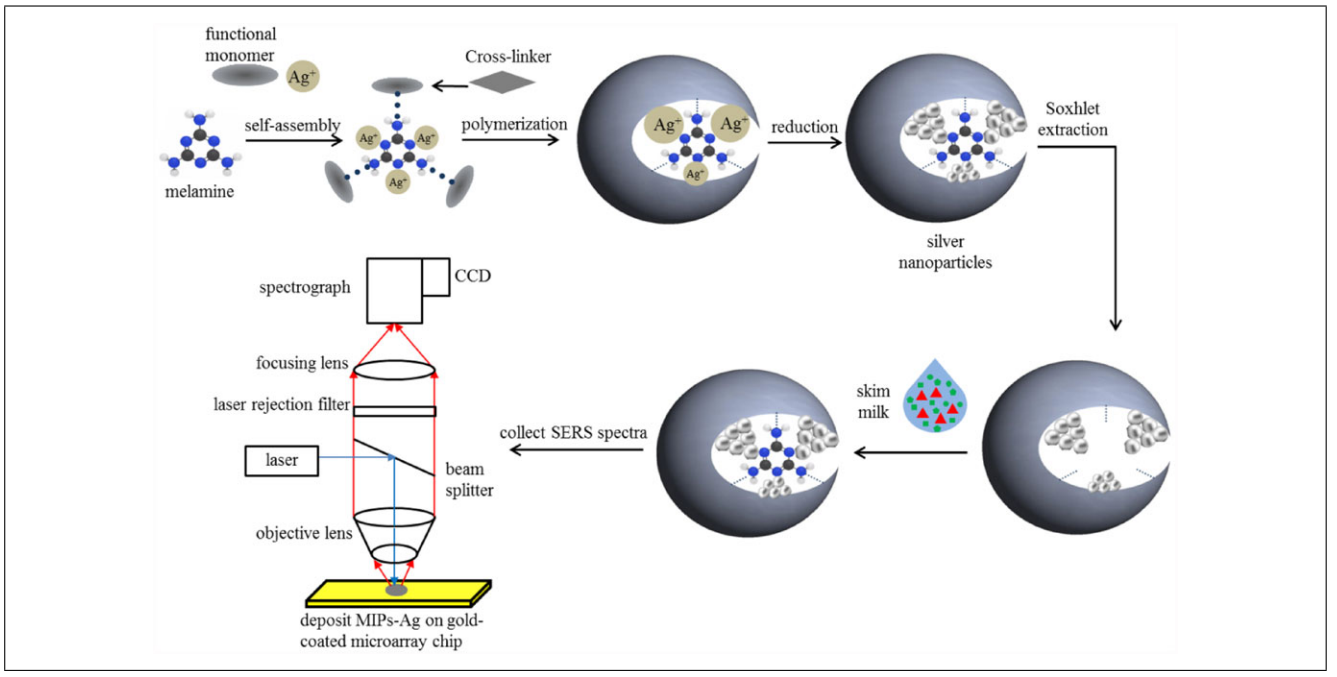

Figure 1–Schematic illustration of "one-step" MIPs-SERS sensor for the detection of melamine in skim milk samples. CCD, charge coupled device; MIPs, molecularly imprinted polymers; SERS, surface enhanced Raman spectroscopy.

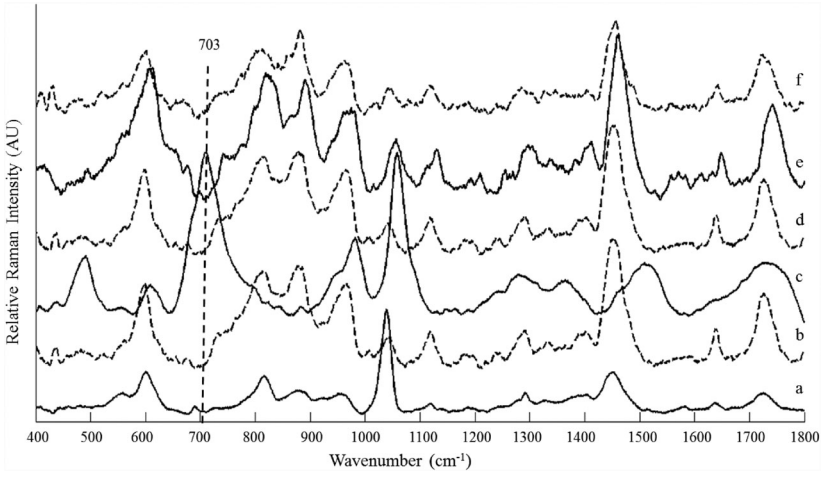

Figure 2–Representative Raman spectra of MIPs-AgNPs and NIPs-AgNPs before and after the reduction of Ag^+ and after Soxhlet extraction. Solid lines represent spectra of MIPs-AgNPs, and dashed lines represent spectra of NIPs-AgNPs. a–f: MIPs-AgNPs before reduction, NIPs-AgNPs before reduction, MIPs-AgNPs after reduction, NIPs-AgNPs after reduction, MIPs-AgNPs after Soxhlet extraction, NIPs-AgNPs after Soxhlet extraction.

0.5 mL methanol, melamine was eluted out by 1 mL methanol with 5% ammonium hydroxide. The eluent was evaporated to dryness and redissolved in 0.2 mL methanol. The recovery of melamine was evaluated by HPLC-DAD. This pretreatment process took approximately 15 min in total.

HPLC conditions

HPLC analysis was performed on an Agilent 1100 series HPLC system and DAD was set at a wavelength of 240 nm. Samples (2 μL) were injected into a hydrophilic interaction liquid chromatography (HILIC) column (Phenomenex Luna HILIC, 3 μm, 2 mm × 100 mm, Torrance, Calif., U.S.A.) at 30 °C. Each sample was tested in triplicate. The mobile phase was 0.1 M ammonium acetate – acetonitrile (10:90, v/v) with the flow rate of 0.2 mL/min. The total running time for melamine standard solution was 10 min while for each skim milk sample was 22 min.

MIPs-AgNPs extraction

An aliquot of 2.5 mg MIPs-AgNPs was mixed with 0.5 mL melamine tap water solution or pretreated skim milk samples. After horizontally shaking for 5 min, the mixture was centrifuged at 12500 × g for 1 min. The supernatant was discarded and the pellet was dried before depositing onto the gold-coated microarray chip for SERS spectral collection.

Raman spectroscopic instrumentation

A confocal micro-Raman spectroscopic system coupled with a 785 nm near-infrared laser (25 mW incident laser power) was used for SERS spectral collection. The system contains a spectrometer (Renishaw, Gloucestershire, U.K.) with an entrance aperture of 50 μm, a focal length of 300 mm, and a 1200 line/mm grating. SERS signal features were recorded by a charge coupled device (CCD) array detector (578 by 385 pixel), with a pixel size of 22 μm.

SERS spectra were collected from samples illuminated by the incident laser through the Leica microscope (Leica Biosystems, Wetzlar, Germany) equipped with a 50× Nikon objective (NA = 0.75, WD = 0.37). The spectra of each sample were collected with an exposure time of 10 s. All experiments were conducted at least in triplicate.

Spectral analysis and chemometric models

Vancouver Raman Algorithm software (BC Cancer Agency & University of British Columbia, Vancouver, BC, Canada) was applied for 6-order of polynomial fit baseline correction and smoothing (11-Size Boxcar algorithm) of collected SERS spectra. These spectral preprocessing reduced spectral noise and increased spectral signal-to-noise ratio (Feng and others 2013). MATLAB R2014a (the MathWorks, Inc., Natick, Mass., U.S.A.) software was used to construct unsupervised principal component analysis (PCA) models to differentiate various samples based on the SERS intensity of wavenumber from 650 to 750 cm^{-1}, while supervised partial least squares regression (PLSR) models were also investigated to correlate melamine concentrations and the corresponding SERS intensities for the quantification of melamine in water and milk.

Results and Discussion

Synthesis of MIPs-AgNPs

Schematic illustration of the synthesis of MIPs-AgNPs is shown in Figure 1. Based on our recent publication (Hu and others 2015), MIPs with specific affinity to melamine had been successfully synthesized by bulk polymerization. Previous research conducted by Liu and others (2011) validated the feasibility of incorporating MIPs and SERS-active substrate by addition of $AgNO_3$ as the AgNPs precursor during the synthesis of MIPs. The integrated MIPs-AgNPs was then fabricated and used to bind melamine, followed by illumination using Raman spectrometer to detect trace level of melamine.

Figure 2 shows the representative Raman spectra of MIPs-AgNPs and NIPs-AgNPs before and after the reduction of Ag^+ (that is AgNPs precursor) and Soxhlet extraction, respectively. Before adding $NaBH_4$ for the reduction of Ag^+, the Raman spectral intensities were relatively weak because of the faint Raman inelastic scattering. Thus, no melamine feature band was found. However, after the formation of AgNPs, the featured melamine band at 703 cm^{-1} (that is ring-breathing mode II of triazine ring) appeared in the spectra of MIPs-AgNPs. According to the principle of SERS, Raman scattering can be enhanced significantly only when the molecule approaches to the surface of SERS-active substrate, because electromagnetic field generated by the localized surface plasmon resonance shows distance dependency (He and others 2011a). With the increases of distance between molecule and SERS-active substrate, the enhancement effect decreases with the squares of distance. Generally, only molecules located within 10 nm to the surface of SERS-active substrates have significantly enhanced Raman scattering signals. Therefore, the appearance of melamine feature band in the spectrum of MIPs-AgNPs after the reduction validated the adjacent location of AgNPs and cavities for melamine. Moreover, the disappearance of melamine feature band in the spectrum of MIPs-AgNPs after Soxhlet extraction

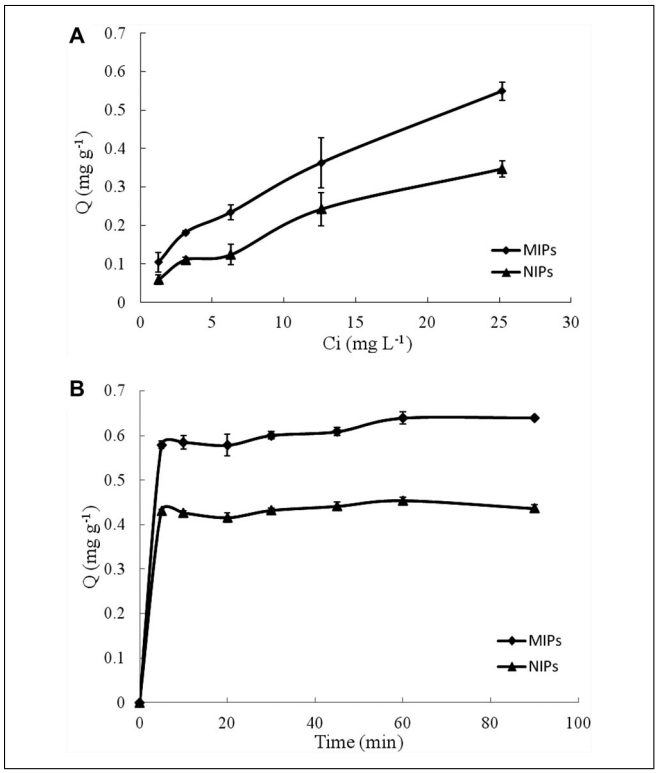

Figure 3–(A) Static binding isotherm of MIPs-AgNPs and NIPs-AgNPs for melamine. (B) Kinetic binding isotherm of MIPs-AgNPs and NIPs-AgNPs (C_i: 12.6 mg/L). C_i: initial concentration of melamine; Q: binding capacity; error bars indicated standard deviation ($N = 3$).

demonstrated the complete removal of template molecule (that is melamine). Variations found between the spectra can be attributed to the inhomogeneity of the location of AgNPs in MIPs-AgNPs, leading to the differences in chemical structures being enhanced by SERS effect. Except some minor variations in the intensity of some bands of NIPs-AgNPs spectra, no obvious change could be found for NIPs-AgNPs spectra before and after the reduction and Soxhlet extraction, indicating that Raman scattering signals contributed by the polymers themselves had no negative effect on the detection of melamine.

The formation of AgNPs can be further validated by the band at 400 nm in UV-Vis spectra, which is contributed by the surface plasmon resonance of AgNPs of 40 nm in size (Song and others 2009; Liu and others 2011). Figure S1 shows the representative UV-Vis spectra of MIPs synthesized for the "two-step" sensor and MIPs-AgNPs before and after the reduction. MIPs-AgNPs before the reduction of Ag^{+} shows stronger absorbance at 400 nm compared to the "two-step" MIPs without the addition of AgNPs precursor, demonstrating the partial formation of AgNPs during the polymerization of "one-step" MIPs-$AgNO_3$. However, after the reduction, the absorbance at 400 nm further increased and the band became sharper, due to the enhanced surface plasmon resonance by the formation of more AgNPs.

Characterization of MIPs-AgNPs

After confirming the complete removal of template molecule, static and kinetic adsorption capacity tests were conducted for the validation of specific affinity of MIPs-AgNPs toward melamine and evaluation of equilibration rate, respectively. The binding capacity of NIPs-AgNPs was contributed by nonspecific binding that adsorbs analyte without recognizing its exact structure, while MIPs-AgNPs bond analyte by both specific and nonspecific bindings. Thus, MIPs-AgNPs has specific affinity toward analyte if its adsorption capacity is higher than NIPs-AgNPs. The results of static adsorption capacity test (Figure 3A) indicated that MIPs-AgNPs exhibited higher adsorption capacity than NIPs-AgNPs regardless of the initial melamine concentration. In sum, successful imprint of chemical and physical properties of melamine in MIPs-AgNPs was realized.

Comparing with the "two-step" MIPs or NIPs synthesized previously in our laboratory (Hu and others 2015), these "one-step" MIPs-AgNPs or NIP-AgNPs showed similar adsorption capacities at the initial melamine concentration of 6.3 ppm (Figure S2). For the same amount of "one-step" and "two-step" polymers, the addition of AgNPs reduced the amount of imprinted polymers that can bind to melamine. Therefore, the identity of "one-step" and "two-step" polymers in terms of adsorption capacity

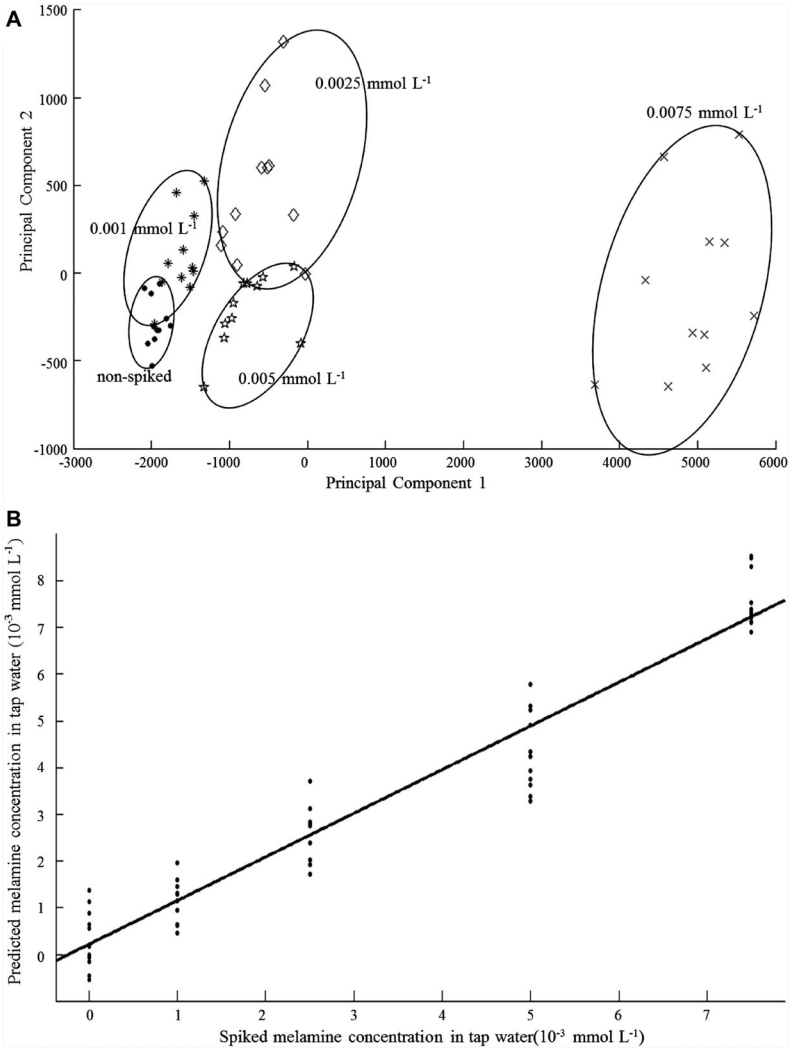

Figure 4–(A) Representative PCA model for tap water samples spiked with different concentrations of melamine. Different markers represent different melamine concentrations: cross sign, 0.0075 mmol/L; pentagram, 0.005 mmol/L, diamond, 0.0025 mmol/L; asterisk, 0.001 mmol/L; and dot, nonspiked samples. (B) Representative PLSR calibration model for tap water samples spiked with different concentration of melamine. ($N = 11$)

Table 1–Parameters of partial least squares regression (PLSR) models for the determination of melamine in tap water and skim milk.

Sample matrices	N^a	factors	SEC[b]	R^2	SECV[c]	R^2_{CV}
Tap water	55	6	0.0027	0.94	0.0024	0.75
Skim milk	45	7	0.036	0.97	0.033	0.80

[a]*N*, number of spectra for calibration.
[b]SEC, standard error of calibration.
[c]SECV, standard error of cross-validation (5-fold).

indicates that AgNPs promoted the adsorption behaviors of polymer itself, which might be associated with the electrostatic interactions between melamine and AgNPs.

Figure 3B shows the results of kinetic adsorption capacity test. Both MIPs-AgNPs and NIPs-AgNPs reached to the equilibrium within 5 min and remained stable for longer incubation time. However, NIPs-AgNPs exhibited lower adsorption capacity compared to MIPs-AgNPs, further validating the specific affinity of MIPs-AgNPs toward melamine. The short equilibration time indicates the potential for rapid recognition and extraction of melamine from real sample matrices.

The selectivity of MIPs-AgNPs toward melamine analogue (for example, cyanuric acid) was not conducted because false positive results could not be acquired by applying SERS for detection. SERS reveals the chemical structure of analytes and provides fingerprinting spectral features to identify chemicals. The wavenumbers of featured SERS bands of melamine and cyanuric acid are different (He and others 2008; Liu and others 2010), resulting in differentiation of melamine and cyanuric acid during detection. Therefore, even if MIPs-AgNPs lacks the capability to remove cyanuric acid during sample pretreatment, SERS spectral features can be used to further distinguish these compounds, avoiding false positive results. Besides, as a metabolite of melamine, cyanuric acid also possesses potential detriment to human (Tyan and others 2009). The false positive results associated with cyanuric acid are also of great significance to assure food safety.

Extraction and determination of melamine in tap water by MIPs-AgNPs

Tap water was used as a simple real sample matrix, spiked with melamine at various concentrations, mixed with MIPs-AgNPs for 5 min, and then illuminated by Raman incident laser for SERS spectral collection. The appearance of the featured melamine SERS band after 5 min incubation (Figure S3) demonstrated the rapid binding attribute of MIPs-AgNPs toward melamine in tap water. Figure 4 shows the representative 2-dimensional PCA model constructed with spectral features of wavenumber from 650 to 750 cm^{-1}. Samples with the same melamine concentration were clustered together. Although scatterings of samples with the same melamine concentration were observed on PC2, the variations could be neglected because PC2 only explained 2.52% of the total variances, while PC1 contributed to 93.45% of the total variances. In addition, PCA loading plot of PC1 (Figure S4) validated that the variances between samples with different melamine concentrations were mainly attributed to the featured melamine SERS band at 703 cm^{-1}. The similarity of PC1 values for samples with the same melamine concentration validated good SERS spectral reproducibility. However, overlaps of SERS spectral features were found between samples with 0.001 mmol/L and nonspiked sample, and between 0.0025 and 0.005 mmol/L samples. PLSR calibration model with 6 latent variables was constructed using the spectral range of 1800 to 400 cm^{-1} for quantification of melamine in tap water (Figure 4) and 5-fold cross-validation was also applied to avoid overfitting of PLSR calibration model. Model parameters are summarized in Table 1. The significant decrease from R^2 to R^2_{cv} represents the overfitting of the PLSR calibration model. LOD and LOQ were determined as 3 times and 10 times the standard deviation of tap water samples with no spiking of melamine (that is $LOD = 3\sigma_{blank}$ and $LOQ = 10\sigma_{blank}$) (Thomsen Schatzlein and Mercuro 2003; Strickland and Batt 2009), and the results are 0.0019 and 0.0064 mmol/L, respectively. With the low R^2 and R^2_{cv}, this model was not feasible for accurate quantification of melamine in tap water. However, the LOD and LOQ was below the maximum tolerance by regulation (that is 2.5 ppm = 0.020 mmol/L) demonstrating the potential applicability.

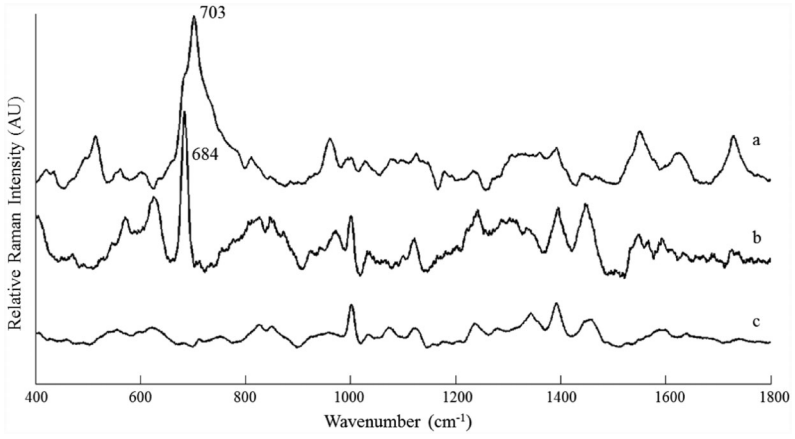

Figure 5–Representative SERS spectral features of MIPs-AgNPs with 0.01 mmol/L melamine in methanol as positive control (a), 0.017 mmol/L melamine in skim milk (b) and nonspiked skim milk as negative control (c).

Extraction and determination of melamine in milk by MIPs-AgNPs

To investigate the application of this innovative sensor for a more complex food matrix, whole milk was selected in the preliminary study. Whole milk samples spiked with melamine were pretreated with methanol or acetonitrile to remove fat and protein. Syringe filter (2 μm) was used to eliminate the influence of short chain proteins. However, no melamine feature band could be observed even after incubation with MIPs-AgNPs together for 2 h. SPE was used to further remove the food matrices, but no difference was found between the spectra of MIPs-AgNPs after mixing with melamine spiked whole milk and nonspiked whole milk. The specific affinity of MIPs-AgNPs was hindered by whole milk food matrices. The phenomenon could be attributed to the concealing of the specific cavities or the masking of AgNPs by some large molecules. Therefore, skim milk was selected as the food matrix.

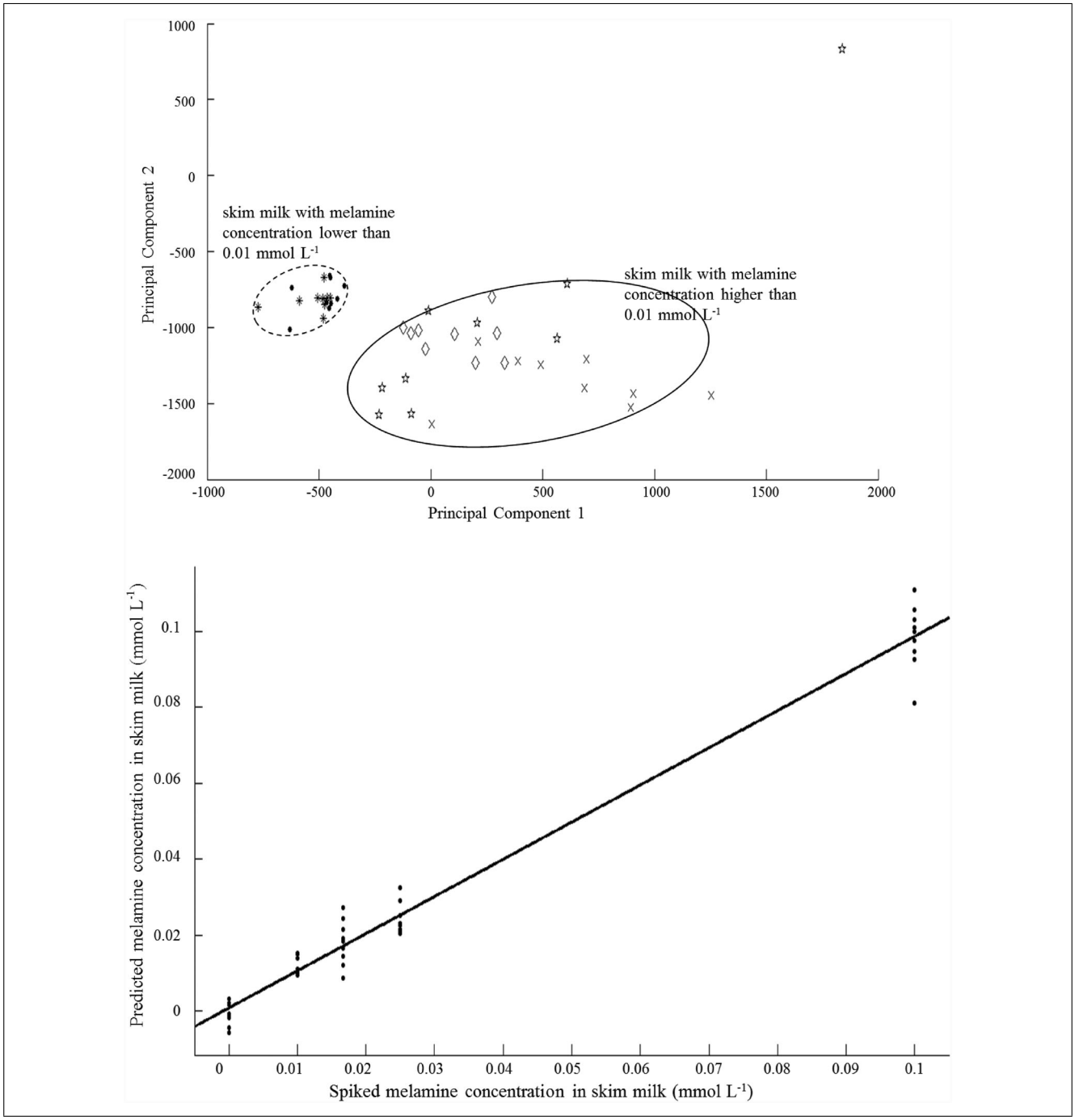

Figure 6–(A) Representative PCA model for skim milk samples spiked with different concentrations of melamine. Different markers represent different melamine concentrations: cross sign, 0.1 mmol/L; pentagram, 0.025 mmol/L, diamond, 0.017 mmol/L; asterisk, 0.01 mmol/L; and dot, nonspiked samples. Cluster circled with dashed line indicates skim milk samples with melamine concentration lower than 0.01 mmol/L. Cluster circled with solid line contains samples with melamine concentration higher than 0.01 mmol/L. (B) Representative PLSR calibration model for skim milk samples spiked with different concentrations of melamine. ($N = 9$).

After spiking with melamine at different concentrations, skim milk samples were firstly pretreated with the commercial silica-based SPE cartridges. Then, the eluents were mixed with MIPs-AgNPs for 5 min followed by SERS spectral collection. The overall analysis could be finished in 25 min. Representative SERS spectra for 0.1 mmol/L melamine in methanol (that is positive control), 0.017 mmol/L melamine in skim milk and nonspiked skim milk (that is negative control) are shown in Figure 5. The featured melamine band in the positive control was identical to the band in MIPs-AgNPs after reduction, as shown in Figure 2. The intensive band at 684 cm^{-1} in the spectrum of 0.017 mmol/L melamine spiked skim milk was assigned to the ring-breathing mode II of triazine ring in melamine. The shift of the melamine feature band was due to SERS effect (Haynes McFarland and Duyne 2005) and changes of melamine structure in different *p*H conditions. Melamine spiked in methanol had *p*H of 5.04, while *p*H of melamine spiked in skim milk was 6.71. As a base itself, melamine acquires more positive charges in lower *p*H conditions; thus the dipole of melamine changes accordingly, leading to different Raman scattering behaviors. Moreover, variations in melamine structure could also change the interaction between melamine and AgNPs, resulting in shift of the wavenumber of melamine feature band. The obvious band in the spectrum of 0.017 mmol/L melamine spiked skim milk compared to the nonspiked samples validated the feasibility of using this MIPs-AgNPs to capture and determine melamine in skim milk.

Representative 2-dimensional PCA model was constructed to differentiate skim milk samples with various melamine concentrations using spectral features between wavenumbers of 650 to 750 cm^{-1} (Figure 6). Loading plot (Figure S5) demonstrates that intensities of band at 683 cm^{-1} contributed most to the overall variation of the spectra, which is associated with the featured melamine band. Forty-five spectra for 5 concentrations of melamine in skim milk were clearly segregated into 2 clusters. Samples with melamine concentrations lower than 0.01 mmol/L were grouped together, while samples with higher concentrations have similar PC scores and located closely to each other, representing the saturation of the sensor. PLSR calibration model (Figure 6) and cross-validation model were also developed and parameters are summarized in Table 1. Compared with the calibration model, the significant lower R^2_{cv} represents overfitting of the calibration model. The LOD and LOQ were calculated according to the formula stated previously and the results are 0.0165 and 0.055 mmol/L, respectively. However, because of the low R^2_{cv}, this representative PLSR calibration model is not ideal to accurately quantify melamine concentration in skim milk. The higher LOD of this MIPs-AgNPs for melamine in skim milk compared to that for tap water is due to the interference from the complex skim milk matrix.

SPE was involved in sample pretreatment because of the interferences by the complex food matrix, leading to increase in time for overall analysis (that is, 25 min) compared to the "two-step" MIPs-SERS sensor (that is, 18 min) (Hu and others 2015). However, the reproducibility of SERS spectra could increase by decorating the specific cavities in MIPs with SERS-active substrate (that is, AgNPs). In the "two-step" sensor, eluents with melamine were deposited onto Ag dendrite nanostructure for SERS measurement. The location of melamine on SERS-active substrate is random, and not all of which are located in the electromagnetic field. Thus, spots of the enhanced melamine Raman signals require extensive time to identify. On the contrary, melamine was adsorbed in the specific cavities using the integrated MIPs-AgNPs and adjacent AgNPs provide electromagnetic field to enhance the Raman signals. By modifying the synthesis of this conjugated MIPs-AgNPs, or by integrating more effective SERS-active substrates, the sample pretreatment procedures can be further simplified, making this technique more appealing for food industry and government laboratory.

Conclusions

This "one-step" MIPs-SERS sensor conjugating MIPs and AgNPs during polymerization showed feasibility for specific separation and detection of trace level melamine in tap water and milk, with the LOD of 0.0019 and 0.0165 mmol/L, and LOQ of 0.0064 and 0.055 mmol/L, respectively. Based on the PLSR models, this proposed sensor failed to accurately quantify melamine in tap water and skim milk. The overall analysis time required for melamine in tap water was 6 min and for skim milk was 25 min. Although this "one-step" MIPs-SERS required longer time to determine melamine in skim milk compared to the previous "two-step" MIPs-SERS for whole milk (that is, 18 min) (Hu and others 2015), the detection was still rapid and the reproducibility of SERS spectra was increased by controlling the distances between melamine and SERS-active substrate, resulting in more efficient detection. Moreover, this conjugated 1 element sensor makes the detection simpler and has the potential for in-field or on-site detection. Thus, this "one-step" MIPs-SERS sensor meets the demands of high-throughput screening and trace level detection of melamine required by food industry and government laboratory.

Acknowledgments

The authors thank Hilda Kisielewski for technical support. This study was supported by Discovery and Engage Funds award to X.L. by Natural Sciences and Engineering Research Council of Canada. X.L. also thanks the support by Mitacs Accelerate Program in Canada.

References

Brown CA, Jeong K-S, Poppenga RH, Puschner B, Miller DM, Ellis AE, Brown SA. 2007. Outbreaks of renal failure associated with melamine and cyanuric acid in dogs and cats in 2004 and 2007. J Vet Diagn Invest 19(5):525–31.

Cheung W, Shadi IT, Xu Y, Goodacre R. 2010. Quantitative analysis of the banned food dye Sudan-1 using surface enhanced Raman scattering with multivariate chemometrics†. J Phys Chem C 114(16):7285–90.

Choo-Smith LP, Edwards HGM Endtz HP, Kros JM, Heule F, Barr H, Puppels GJ. 2002. Medical applications of Raman spectroscopy: from proof of principle to clinical implementation. Biopolymers 67(1):1–9.

Colthup N. 2012. Introduction to infrared and Raman spectroscopy. 2nd ed. Academic Press. New York

Feng S., Gao F, Chen Z, Grant E, Kitts DD, Wang S, Lu X. 2013. Determination of α-tocopherol in vegetable oils using a molecularly imprinted polymers-surface-enhanced Raman spectroscopic biosensor. J Agric Food Chem 61(44):10467–75.

Filazi A, Sireli U, Ekici H, Can H, Karagoz A. 2012. Determination of melamine in milk and dairy products by high performance liquid chromatography. J Dairy Sci 95(2):602–8.

Gao F, Feng S, Chen Z, Li-Chan EC, Grant E, Lu X. 2014. Detection and quantification of chloramphenicol in milk and honey using molecularly imprinted polymers: Canadian penny-based SERS nano-biosensor. J Food Sci 79(12):N2542–9.

Haupt K. 2003. Molecularly imprinted polymers: the next generation. Anal Chem 75(17):376 A–83 A.

Haynes CL, McFarland AD, Duyne RPV. 2005. Surface-enhanced Raman spectroscopy. Anal Chem 77(17):338 A–46 A.

He C, Long Y, Pan J, Li K, Liu F. 2007. Application of molecularly imprinted polymers to solid-phase extraction of analytes from real samples. JBiochem Biophys Methods 70(2):133–50.

He J, Wang S, Fang G, Zhu H, Zhang Y. 2008. Molecularly imprinted polymer online solid-phase extraction coupled with high-performance liquid chromatography– UV for the determination of three sulfonamides in pork and chicken. J Agric Food Chem 56(9):2919–25.

He L, Liu Y, Lin M, Awika J, Ledoux D, Li H, Mustapha A. 2008. A new approach to measure melamine, cyanuric acid, and melamine cyanurate using surface enhanced Raman spectroscopy coupled with gold nanosubstrates. Sens Instrument Food Qual Safety 2(1):66–71.

He L, Lamont E, Veeregowda B, Sreevatsan S, Haynes CL, Diez-Gonzalez F, Labuza TP. 2011a. Aptamer-based surface-enhanced Raman scattering detection of ricin in liquid foods. Chem Sci 2(8):1579–82.

He L, Rodda T, Haynes CL, Deschaines T, Strother T, Diez-Gonzalez F, Labuza TP. 2011b. Detection of a foreign protein in milk using surface-enhanced Raman spectroscopy coupled with antibody-modified silver dendrites. Anal Chem 83(5):1510–3.
Holthoff EL, Stratis-Cullum DN, Hankus ME. 2011. A nanosensor for TNT detection based on molecularly imprinted polymers and surface enhanced Raman scattering. Sensors 11(3):2700–14.
Hu Y, Feng S, Gao F, Li-Chan EC, Grant E, Lu X. 2015. Detection of melamine in milk using molecularly imprinted polymers—surface enhanced Raman spectroscopy. Food Chem 176:123–9.
Ingelfinger JR. 2008. Melamine and the global implications of food contamination. N Engl J Med 359(26):2745–8.
Kantarovich K, Tsarfati I, Gheber LA, Haupt K, Bar I. 2010. Reading microdots of a molecularly imprinted polymer by surface-enhanced Raman spectroscopy. Biosens Bioelectr 26(2):809–14.
Li-Chan ECY. 1996. The applications of Raman spectroscopy in food science. Trends Food Sci Technol 7(11):361–70.
Li X, Feng S, Hu Y, Sheng W, Zhang Y, Yuan S, Lu X. 2015. Rapid detection of melamine in milk using immunological separation and surface enhanced Raman spectroscopy. J Food Sci 4(1):13–9.
Liu B, Lin M, Li H. 2010. Potential of SERS for rapid detection of melamine and cyanuric acid extracted from milk. Sens Instrument Food Qual Safety 4(1):13–9.
Liu B, Zhou P, Liu X, Sun X, Li H, Lin M. 2013. Detection of pesticides in fruits by surface-enhanced Raman spectroscopy coupled with gold nanostructures. Food Bioproc Technol 6(3):710–8.
Liu P, Liu R, Guan G, Jiang C, Wang S, Zhang Z. 2011. Surface-enhanced Raman scattering sensor for theophylline determination by molecular imprinting on silver nanoparticles. Analyst 136(20):4152–8.
Lombardo-Agüí M, García-Campaña AM, Gámiz-Gracia L, Blanco CC. 2010. Laser induced fluorescence coupled to capillary electrophoresis for the determination of fluoroquinolones in foods of animal origin using molecularly imprinted polymers. J Chromatogr A 1217(15):2237–42.
Lu X, Huang Q, Miller WG, Aston DE, Xu J, Xue F, Konkel ME. 2012. Comprehensive detection and discrimination of Campylobacter species by use of confocal micro-Raman spectroscopy and multilocus sequence typing. J Clin Microbiol 50(9):2932–46.
Lu X, Samuelson DR, Xu Y, Zhang H, Wang S, Rasco BA, Konkel ME. 2013. Detecting and tracking nosocomial methicillin-resistant Staphylococcus aureus using a microfluidic SERS biosensor. Anal Chem 85(4):2320–7.
Pang S, Labuza TP, He L. 2014. Development of a single aptamer-based surface enhanced Raman scattering method for rapid detection of multiple pesticides. Analyst 139(8):1895–901.
Song K, Lee S, Park T, Lee B. 2009. Preparation of colloidal silver nanoparticles by chemical reduction method. Korean J Chem Eng 26(1):153–5.
Strickland AD, Batt CA. 2009. Detection of carbendazim by surface-enhanced Raman scattering using cyclodextrin inclusion complexes on gold nanorods. Anal Chem 81(8):2895–903.
Thomsen V, Schatzlein D, Mercuro D. 2003. Limits of detection in spectroscopy. Spectroscopy 18(12):112–14.
Tyan Y-C, Yang M-H, Jong S-B, Wang C-K, Shiea J. 2009. Melamine contamination. Anal Bioanal Chem 395(3):729–35.
Wang S, Xu Z, Fang G, Duan Z, Zhang Y, Chen S. 2007. Synthesis and characterization of a molecularly imprinted silica gel sorbent for the on-line determination of trace Sudan I in chilli powder through high-performance liquid chromatography. J Agric Food Chem 55(10):3869–76.
Wu Y, Zhao Y, Li J. 2009. A survey on occurrence of melamine and its analogues in tainted infant formula in China. Biomed Environ Sci 22(2):95–9.
Xie Y, Li Y, Niu L, Wang H, Qian H, Yao W. 2012. A novel surface-enhanced Raman scattering sensor to detect prohibited colorants in food by graphene/silver nanocomposite. Talanta 100:32–7.
Xu X, Ren Y, Zhu Y, Cai Z, Han J, Huang B, Zhu Y. 2009. Direct determination of melamine in dairy products by gas chromatography/mass spectrometry with coupled column separation. Anal Chim Acta 650(1):39–43.
Yakala GK, Wielinga PY, Suarez M, Bunschoten A, van Golde JM, Arola L, Heeringa P. 2013. Effects of chocolate supplementation on metabolic and cardiovascular parameters in ApoE3L mice fed a high-cholesterol atherogenic diet. Mol Nutr Food Res 57(11):2039–48.
Yang H, Zhou W, Guo X, Chen F, Zhao H, Lin L, Wang X. 2009. Molecularly imprinted polymer as SPE sorbent for selective extraction of melamine in dairy products. Talanta 80(2):821–5.
Zheng X, Yu B, Li K, Dai Y. 2012. Determination of melamine in dairy products by HILIC-UV with NH 2 column. Food Contl 23(1):245–0.

Supporting Information

Additional Supporting Information may be found in the online version of this article at the publisher's website:

Figure S1. Representative UV-Vis spectra of "two-step" MIPs, "one-step" MIPs-AgNPs before and after the reduction of Ag+. Solid line: two-step MIPs; dotted line: MIPs-AgNPs before the reduction of Ag+; dashed line: MIPs-Ag-NPs after the reduction of Ag+.

Figure S2. Comparison of the adsorption capacity of "one-step" and "two-step" MIPs and NIPs (Ci: 6.3 mg/L). Means with different letters are significantly different (one-tail paired *t*-test, $\alpha = 0.05$). Q: binding capacity; Ci: initial concentration of melamine.

Figure S3. Representative SERS spectral features of MIPs-AgNPs with 0.0075 mmol/L melamine in tap water.

Figure S4. Loading plot of the representative PCA model for tap water samples spiked with different concentrations of melamine. PC1 represents 93.45% variances.

Figure S5. Loading plot of the representative PCA model for skim milk samples spiked with different concentrations of melamine. PC1 represents 45.69% variances and PC2 represents 25.11% variances.